



Advance and prospect of metal-organic frameworks for perovskite photovoltaic devices

Xiao Liang^{a,b}, Xianfang Zhou^{a,b}, Chuangye Ge^b, Haoran Lin^b, Soumitra Satapathi^c, Quanyao Zhu^{a,**}, Hanlin Hu^{b,*}

^a State Key Laboratory of Advanced Technology for Materials Synthesis and Processing, School of Materials Science and Engineering, Wuhan University of Technology, Wuhan, 430070, PR China

^b Hoffmann Institute of Advanced Materials, Shenzhen Polytechnic, 7098 Liuxian Boulevard, Shenzhen, 518055, PR China

^c Department of Physics, Indian, Institute of Technology, Roorkee, Uttarakhand, 247667, India

ABSTRACT

Improving the long-term stability is now one of the most critical challenges in perovskite photovoltaic devices. Recently, metal-organic frameworks (MOFs) with appreciable chemical and moisture stabilities are increasingly used in optoelectronics devices. The introduction of MOFs into perovskite solar cells has paved an innovative way to address the stability issue. Consequently, the combination of perovskite photovoltaics with MOFs has drawn significant research interest in the perovskite community not only due to the enhanced stability but also for the improved photovoltaic performance resulting from the reduced defect concentration, increased charge-carrier transport, and effective energy-band alignment. This review focuses on the development of MOF-assisted perovskite photovoltaic devices and systematically summarizes the recent progress in this new type of optoelectronic device upon the combination of MOFs and perovskite photovoltaics. We have critically analyzed various functions of MOFs, including individual interlayer, a modifier of the interlayer, and MOFs/perovskite heterojunction. Furthermore, we provide a roadmap about the potential challenges and prospects of MOF-based perovskite solar cells.

1. Introduction

Perovskite solar cells (PSCs) with power conversion efficiencies (PCEs) reached 25.7% [1], showing great promise for scale-up and future commercialization due to relatively simple and low-cost solution processes [2–6]. However, the long-term stability of PSCs is the most urgent challenge which needs to be solved before the deployment of perovskite photovoltaic technology [7–12]. Huge research work in this community has evidenced that the poor stability of polycrystalline perovskite materials can be caused by UV radiation, moisture, oxygen, and so on [13–15]. Tremendous effort has been made to address those issues regarding the instability issue, including mixed dimensional architecture [16,17], composition engineering, and encapsulation technology [18,19], which are especially effective to solve those external factors, including oxygen and water, while the poor stability limited by the intrinsic ionic polycrystalline nature with inevitable high defect states and grain boundaries remains quite challenging [20–23]. These defects are responsible for local charge accumulation, accelerated ion migration, and the initial invasion of moisture or oxygen, ultimately causing device instability issues [24]. Diverse approaches have been

reported to enhance the stability of perovskite materials themselves with suppressed defect states, such as fabrication process optimization, grain boundary passivation, doping, and so on [25–27].

Recently, nanoscale metal-organic frameworks (MOFs) have drawn increasing attention in the perovskite photovoltaic community due to their moistly, chemically, and thermally stable nanostructure with significantly improved PSCs stability as well as enhanced device performance [28–30]. MOFs are a kind of crystalline microporous materials composed of a regular array of positively charged metal ions periodic connected by organic “linker” molecules [31]. Their structure is flexible and can be tuned by variation of the nature of the metal cation and linkers and by post-synthesis modification [32]. The key development of MOFs porous materials was marked by the introduction of secondary building units (SBUs) [33]. The polynuclear properties result in the formation of extended porous networks and thus the synthesis of stable and rigid structures [34]. They are known for their high surface area, considerable pore volume, high concentration of active metal sites, flexible structure, tunable pore diameters, and controllable topology [35–38]. The excellent stability combined with high specific surface area and facile solution processability has extended its application from

* Corresponding author.

** Corresponding author.

E-mail addresses: cglamri@whut.edu.cn (Q. Zhu), hanlinhu@szpt.edu.cn (H. Hu).

<https://doi.org/10.1016/j.orgel.2022.106546>

Received 10 April 2022; Received in revised form 25 April 2022; Accepted 29 April 2022

Available online 5 May 2022

1566-1199/© 2022 Elsevier B.V. All rights reserved.

gas storage [39], gas separation [40], and catalysis [41] to optoelectronic devices, aimed to improve the device stability [27]. Moreover, these incorporated MOFs could provide various functionalities in the device by controlling the constituent metal ions and organic linkers according to their applications [42]. Since its first publication in 2014 [43], there has been a number of papers on MOF-PSCs with remarkably improved device stability and optoelectronic performance [28–30].

At present, the application of MOFs in PSCs can be classified into the following situations as illustrated in Fig. 1: (a) MOFs serving as the electron transport layer (ETL) or embedded inside the ETL; (b) MOFs embedded inside the hole transport layer (HTL); (c) MOFs mixed with perovskite materials to prepare MOFs/perovskite heterojunction; (d) MOFs on the interface as an interfacial modification. Alexandr et al. first introduced MOF into ETL of PSCs. The ETL of porous TiO₂-MOF shows high carrier mobility and stability [43]. Chang and co-workers first report was incorporating MOF crystals into PSCs. The small size of MOF-525 acts as a regular scaffold to allow perovskite crystallization inside; the standard scaffold provides an ordered order arrangement of perovskite crystallites during the initial stage of crystallization [28]. Moreover, Wu and co-workers introduced a 2D-MOF at the perovskite/cathode interface. The 2D-MOF used Zr (IV) ions to engage selectively. The complex carboxyl groups allow dense free-standing thiol arrays to be built around the Zr (IV)-oxo cluster to capture most of the Pb²⁺ leaked from the degraded PSCs by forming water-insoluble solids [29]. Table 1 detailed summarizes the collected MOFs comprising various metal ions and organic linkers in the perovskite photovoltaic research area. This review comprehensively summarizes the application and development of MOF in PSCs in recent years. Meanwhile, we will discuss how the marriage of perovskite and MOF crystals brings new material design and functionality evolvments. In the end, the prospects and further developments of MOF in PSCs will be further proposed and discussed.

2. MOFs-modified ETL of PSCs

The electron transport layer (ETL), playing a significant role in electron transfer and hole blocking, is crucial for obtaining efficient

solar cells [54]. Titanium oxide (TiO₂) is a widely utilized n-type material as ETL in PSCs, resulting from its tunable electronic properties, suitable energy level with perovskite, inherent transparency, and low cost [55]. However, TiO₂ has relatively low conductivity, electron mobility, and many defects such as oxygen vacancies metal interstitials at surface and grain boundaries, which are unfavorable for the electron collection transport and result in high recombination rates of photo-generated carriers [56]. Some groups utilized Ti-MOF to prepare porous TiO₂ as ETL to solve this problem. Alexandr and co-workers prepared the first depleted heterojunction TiO₂-MOF-based PSCs by a single-step hydrothermal synthesis. Fig. 2(a) shows the structure of the photoactive TiO₂-MOF composite and a schematic diagram of TiO₂-MOF-based solar cell structures. Three-dimensional (3D) perovskite structures in contact with highly porous TiO₂-MOF coatings possess several significant advantages, such as a large absorption coefficient, high carrier mobility, and high stability. The device shows a PCE of 6.4% [43]. Hou et al. synthesized porous hier-TiO₂ nanostructures by sintering MIL-125(Ti) of MOFs as ETL of PSCs. The ordered hier-TiO₂ nanostructures were coated on a compact TiO₂ layer to form a quasi-mesoscopic (QM) scaffold with scattered distribution, offering sufficient space for the ordered growth of perovskite grains. As shown in Fig. 2(b), The QM-PSCs show a champion PCE of 16.56%, much higher than that of M-PSCs (11.38%) with conventional TiO₂ nanoparticles and P-PSCs with compact TiO₂ layer (6.07%). Moreover, the PCE of QM-PSCs and M-PSCs remains 47% and 22% of their initial value after 30 days of aging in the air [44]. Li and co-workers successfully prepared a novel mesoporous anatase TiO₂ nanocrystalline as ETL of PSCs by sintering the NH₂-MIL-125. The TiO₂ exhibits an appropriate work function, which matches relatively better with the conduction band of perovskite and shows a PCE of 13.49% [57].

In addition, traditional commercial TiO₂ also has the problem of extensive bandgap energy (approximately 3.3 eV). Doping with metals is an effective pathway to reduce the bandgap of TiO₂, which enhances the absorption of sunlight and the extraction of electrons from the perovskite layer [58]. Hguyen and co-workers successfully prepared Co-doped Ti-MOF as an ETL by a solvothermal method. They introduced Co into the TiO₂ ETL, which considerably reduces the bandgap energy of TiO₂,

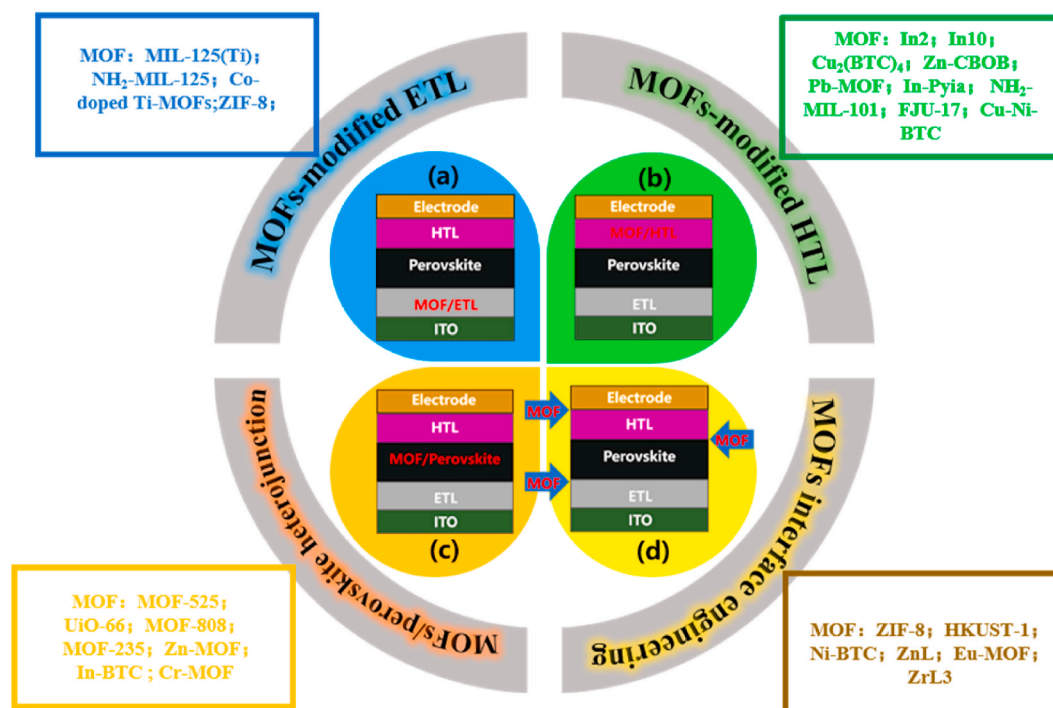


Fig. 1. Various applications of MOFs in perovskite photovoltaic devices have been reported so far.

Table 1

The reported MOFs with those comprising various metal ions and organic linkers in the perovskite photovoltaic research area.

MOFs	Year	Metal Ions	Organic "linker"	Ref.
MIL-125	2017	Ti		[44]
ZIF-8	2020	Zn		[45]
In2	2017	In		[46]
Cu-BTC	2019	Cu		[47]
Zn-CBOB	2021	Zn		[48]
In-Pyia	2020	In		[49]
FJU-17	2020	In		[50]
Ni-BTC	2020	Ni		[51]
ZnL	2021	Zn		[52]
Eu-MOF	2021	Eu		[53]
ZrL ₃	2021	Zr		[29]
MOF-525	2015	Zr		[28]
UIO-66	2019	Zr		[30]
MOF-808	2019	Zr		[30]

leading to increased light absorption. More importantly, doping with Co facilitates the generation of massive distortions and the accompanying defects resulting from the presence of Co atoms in TiO₂ lattices. Finally, the Co-doped Ti-MOF-based PSCs exhibit a PCE of 15.75% [59].

The preparation of TiO₂ often requires high-temperature processing, which significantly limits its flexible application. Ryu et al. synthesized nanocrystalline Ti-based MOF (nTi-MOF) particles as ETLs in PSCs (6 nm in diameter) under room-temperature conditions. Fig. 3(a) shows a synthetic protocol schematic for nanocrystalline Ti-MOF (nTi-MOF) and a flexible PSC device structure with nTi-MOF/PCBM as ETL. Involving [6,6]-phenyl-C61-butyric acid (PCBM) into the nTi-MOF ETL enables efficient electron transfer and suppresses the direct contact of perovskite and electrode. It shows champion PCEs of 18.94% and 17.43% for rigid and flexible devices, respectively. Furthermore, the promising durability was retained in up to 700 bending cycles, showing a PCE of 15.43%. This report provides practical ideas for large-scale flexible PSCs [60]. ZnO is another widely used ETL in PSCs due to its low cost and abundance in nature reserves [61]. Zhang and co-workers adopt MOF-derived (ZIF-8) zinc oxide (MZnO) as an ETL for PSCs for the first time. As shown in Fig. 3(b), MZnO polyhedrons present a dodecahedral morphology with many pores. Large-size MZnO particles could serve as light scattering centers, increasing the light-harvesting efficiency of the perovskite layer. Meanwhile, the porous MZnO can offer a large contact area with the perovskite, where perovskite can adequately penetrate between the polyhedrons and into the pores of MZnO. The MOF-derived ZnO realized improved electron extraction, reduced density of trapped state, and less electron-hole recombination probability. MOF-derived ZnO-based PSCs exhibit a champion PCE of 18.1% coupled with an improved fill factor (FF) of 0.74 and short-circuit current density (*J*_{sc}) of 22.1 mA/cm². The residual PCE of the aged device based on MZnO in 30 days is 77% of its original value [45]. The photovoltaic parameters of the MOFs modified ETL for PSCs are shown in Table 2. At present, the reported PCE of PSCs with MOFs as the ETL is still lagging behind. More research efforts should target on MOF material design with better electron transport and energy level matching to fabricate high-performance perovskite devices.

3. MOFs-modified HTL of PSCs

Although the perovskite material has electron-hole dual transport properties to achieve higher photoelectric conversion efficiency, the role of the hole transport layer (HTL) can't be ignored [62]. The HTL can influence the charge carrier transport and recombination and the perovskite crystallization and device stability [63–65]. The HTL materials mainly play the following four roles: (1) promoting the separation of electrons and holes; (2) forming an ohmic contact with the perovskite layer to collect holes effectively; (3) effectively transporting holes to the electrode; (4) effectively blocking electrons from entering the HTL [66, 67]. At present, many high-efficiency PSCs are held by the 2,2',7,7'-tetrakis-(*N*, *N*-di-4-methoxyphenylamino)-9,9'-spirobifluorene (Spiro-OMeTAD), mainly due to its excellent stability and appropriate energy level [68,69]. However, low intrinsic hole mobility and conductivity restrict its utilization [70]. The combination of MOF and HTL can accelerate the oxidation of Spiro-OMeTAD [71] and the charge transport through band alignment [46]. Li and co-workers first introduced 3D MOF, namely, [In₂(phen)₃Cl₆]-CH₃CN·2H₂O (In2), into Spiro-OMeTAD of PSCs through band alignment engineering. They found that the pinholes were effectively reduced, and the migration into the entire PSC structure can be alleviated simultaneously after introducing In2 in HTL. Meanwhile, In2 also plays a role in enhancing the light absorption of perovskite. Consequently, the PCE improved remarkably from 12.8% to 15.8%, and the device with In2 maintains nearly 78% of its initial PCE after 600 h, while only 69% of initial PCE is obtained in the one without In2 [46]. They further incorporated [In_{0.5}K(3-qlc)Cl_{1.5}(H₂O)_{0.5}]_{2n} (In10) into Spiro-OMeTAD of PSCs. The design idea of the experiment is shown in Fig. 4(a). The intense visible photoluminescence feature of In10 can enhance the light response of

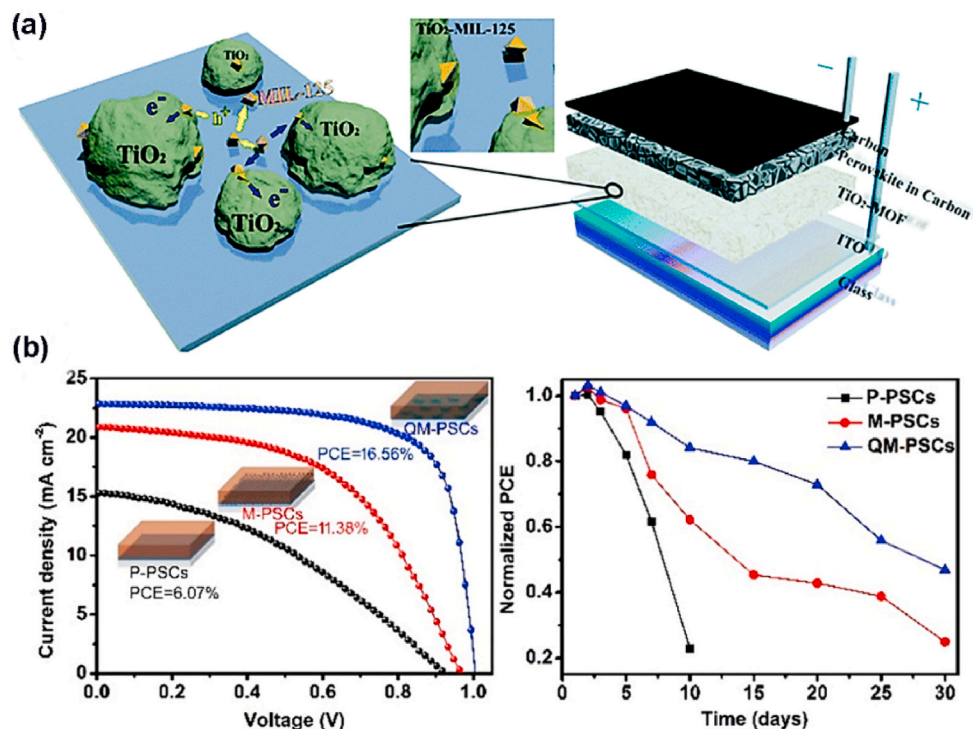


Fig. 2. (a) Visualisation of the structure of the photoactive MOF@TiO₂ composite and the construction of a depleted quasi-bulk heterojunction TiO₂-MOF-based solar cell [43]. (b) J-V characteristic curves and normalized PCE values with aging time for three types of P-PSCs, M-PSCs, and QM-PSCs [44].

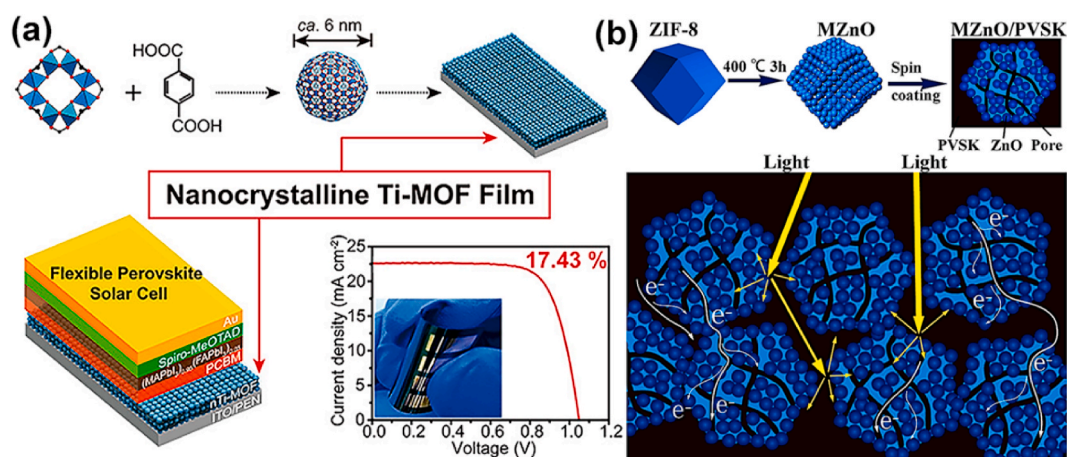


Fig. 3. (a) Schematic presentation of the synthetic protocol for nanocrystalline Ti-MOF (nTi-MOF) and device structure of flexible PSCs based on nTi-MOF/PCBM ETL [60]. (b) The Schematic diagrams of the formation of MOF-Derived ZnO polyhedra and their use as ETL to enhance light harvesting and electrons extraction [45].

perovskite solar cells. As a result, the PCE exhibits 20% enhancement from 14.1 to 17.0% [71]. Dong and co-workers report an efficient hybrid [Cu₂(BTC)₄/3(H₂O)₂]₆[H₃PMo₁₂O₄₀]₂ (POM@Cu-BTC) material for the oxidation of spiro-OMeTAD. The self-assembly of POM and MOFs was employed as an oxidant in the HTL layer for the first time. The POM@Cu-BTC composite exhibits dual functions during chemical doping spiro-OMeTAD (Fig. 4(b)). i). Enhanced hole extraction and transport suppress the charge recombination at the perovskite/HTL interface. ii) The solid-state dopant and its robust framework dramatically reinforce the long-term stability and stability in humid conditions. Finally, a superior FF of 0.80 and enhanced PCE of 21.44% were obtained. The PCE retains approximately 90% of the initial value after long-term storage in ambient environment [47]. Recently, they introduced H₃PMo₁₂O₄₀ into a zirconium-porphyrin-based MOF-545 and employed as effective dopants, which could quantitatively and

controllably oxidize Spiro-OMeTAD under an inert atmosphere, and improve the conductivity and hole mobility accordingly. As a result, the devices show a champion PCE of 21.5% with remarkable long-term air stability, retaining approximately 85% of the initial PCE value for over 1000 h in ambient conditions [72]. Wang et al. developed a highly stable MOF {[Zn(Hcbob)]·(solvent)}_n(Zn-CBOB) with rod topology and Lewis primary sites and employed it as a dopant for the HTL. It is confirmed that Zn-CBOB not only controllably oxidizes Spiro-OMeTAD with improved conductivity but also effectively passivates the surface traps of the perovskite layer by coordinating with Pb²⁺ (Fig. 5(a)), resulting in a remarkable PCE of 20.64%, and the Zn-CBOB-doped device retains beyond 90% of the initial PCE after being stored in the ambient environment (50% RH, 25 °C) for 30 days [48].

Moreover, the research of two-dimensional (2D) MOF and its derived structures in HTL of PSC devices is still scarce. Huang and co-workers

Table 2

Summary of the photovoltaic performance of MOFs-modified ETL of PSCs.

MOF	Device structure	Jsc (mA/ cm ²)	Voc (V)	FF (%)	PCE (%)	Ref.
MIL-125	ITO/MIL-125@TiO ₂ /Perovskite/carbon	10.9	0.85	69.00	6.40	[43]
MIL-125 (Ti)	FTO/hier-TiO ₂ /Perovskite/Spiro-OMeTAD/AgAl	22.81	1.01	71.84	16.56	[44]
NH ₂ -MIL-125	FTO/c-TiO ₂ /N-M-TiO ₂ /Perovskite/ZrO ₂ /carbon	23.52	0.89	64.80	13.49	[57]
Co-doped Ti-MOFs	FTO/c-TiO ₂ /Co-doped TiO ₂ /Perovskite/Spiro-OMeTAD/Au	24.08	1.03	64.95	15.75	[59]
MIL-125 (Ti)	ITO/nTi-MOF/PCBM/Perovskite/Spiro-OMeTAD/Au	23.18	1.08	75.5	18.94	[60]
ZIF-8	FTO/c-TiO ₂ /MnZnO/perovskite/HTM/Ag	22.1	1.11	74	18.1	[45]

incorporated 2D Pb-based MOF with hexagon sheet structure into Spiro-OMeTAD. Compared to a pure Spiro-OMeTAD layer, the composited HTL layer shows a higher hydrophobicity, smoother surface, and upshifted energy levels. The device reveals the higher PCE (13.17%) and stability (54% efficiency of initial value even after nine days in an environment of 30% relative humidity) [73].

As known to all, lithium bis(trifluoromethanesulfonyl)imide (Li-TFSI) and tetra-*tert*-butylpyridine (*t*-BP) are selected as additives to improve the conductivity of Spiro-OMeTAD [74]. However, *t*-BP volatilizes quickly to induce the aggregation, hydration, and ion penetration of lithium salts, thereby seriously impairing the thermal stability of devices [75]. The Li-TFSI can absorb moisture and accelerate the degradation of the perovskite film, resulting in a decrease in the long-term stability of PSCs [76]. Zhou and co-workers developed a novel thermally stable MOF In-Pyria with active pyridyl sites to replace the volatile *t*-BP. In-Pyria fulfills long-term effectiveness to restrain the negative morphological changes of HTL films, attributed to its robust framework and strong coordination effect between pyridine nitrogen atoms and Li⁺ ions. The In-Pyria-modified PSCs show a PCE of 20.26% and still maintain 80.9% of the initial PCE, while it is less than 20% for the *t*-BP-controlled devices (Fig. 5(b)) [49]. The Li-TFSI will absorb moisture and accelerate the degradation of the perovskite film, leading to a decrease in the long-term stability of PSCs. Wang and co-workers constructed a novel dopant Li-TFSI endohedral MOF (namely Li-TFSI@NH₂-MIL-101) to reduce the amount of Li salt and resist the attack from water molecules (Fig. 3(c)). The intense interaction between

ammonium groups (-NH₂) and uncoordinated Pb²⁺ ions would passivate the trap states and inhibit migration at the perovskite/HTL interface, further improving device stability. The cell shows an optimal PCE of 19.01% and stability, retaining over 85% of the optimal PCE after 3600 h storage in the ambient environment [77]. Zhang and co-workers construct a dual-functional layer HTM-FJU-17 by incorporating the (Me₂NH₂)⁺-encapsulated indium-based anionic MOF (FJU-17) as a “capsule” into HTL. The FJU-17 capsule would passivate the organic cation vacancies by releasing (Me₂NH₂)⁺ ion, while its anionic framework can stabilize the positively charged oxidized HTM to enhance hole mobility (Fig. 3(d)). As a result, PSCs exhibit suppressed charge recombination with PCE improvement from 18.32% to 20.34%, and a stable device is obtained with 90% remaining of the original PCE after 1000 h in ambient conditions [50].

Apart from direct adding MOF material as an additive to HTL, some researchers now directly replace Spiro-OMeTAD with MOF material. Hazeghi and co-workers synthesized Cu-Ni MOF as HTL of PSCs by a facile and stepwise solvothermal method. Core-shell CuO@NiO HTL is mainly attributed to the high extraction of charge carrier due to favorable energy level alignment between perovskite and hole transport layer, increase in HTL conductivity, and decrease of defect density in the surface and bulk of HTL. The core-shell CuO@NiO HTL exhibited a greater PCE of 10.11%, and the devices with NiO and CuO@NiO HTLs maintained more than 52% and 60% of their original efficiency after 80 days, respectively [78]. The photovoltaic parameters of the HTL of MOFs applied to PSC are shown in Table 3. Although remarkable progress has been achieved with MOFs as the HTL for PSCs, there is still space for further development, including low-cost, stable MOFs design for a completely replacing of expensive Spiro-OMeTAD material, and so on.

4. MOFs interface engineering of PSCs

MOF materials have also made significant progress in the interface engineering of PSCs. Firstly, MOFs were introduced between the perovskite and ETL layers, which commonly involve building a micro-porous scaffold to regulate the growth of perovskite layers. This improves contact at the ETL/perovskite interface, resulting in enhanced crystallinity and film quality [42]. Shen et al. used MOF (ZIF-8) as an interfacial layer and coated it on the surface of mp-TiO₂ in a PSC system to control the growth of a perovskite crystal layer with a PCE of 16.99% [79]. Chung and co-workers introduced a MOF of ZIF-8 as an interlayer between the mesoporous TiO₂ and the perovskite layer in PSCs. The ZIF-8 solution is dried on the mesoporous TiO₂ layer, which can act as an additional light-absorbing layer at the short-wavelength range for the solar cells, leading to improved performance (PCE of 12.0%) [80]. Ahmadian-Yazdi and co-workers employed zeolitic imidazolate

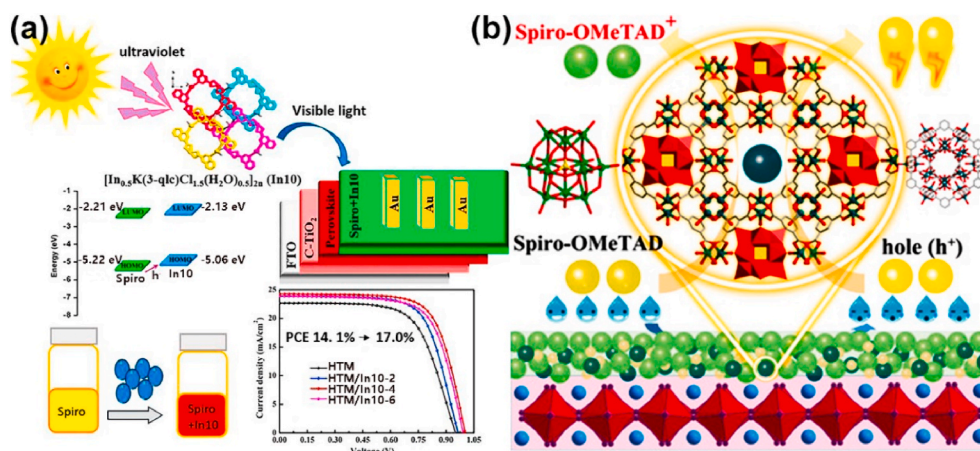


Fig. 4. (a) The design idea of the experiment and J-V curves [71]. (b) Mechanism diagram of POM@Cu-BTC as the HTL [47].

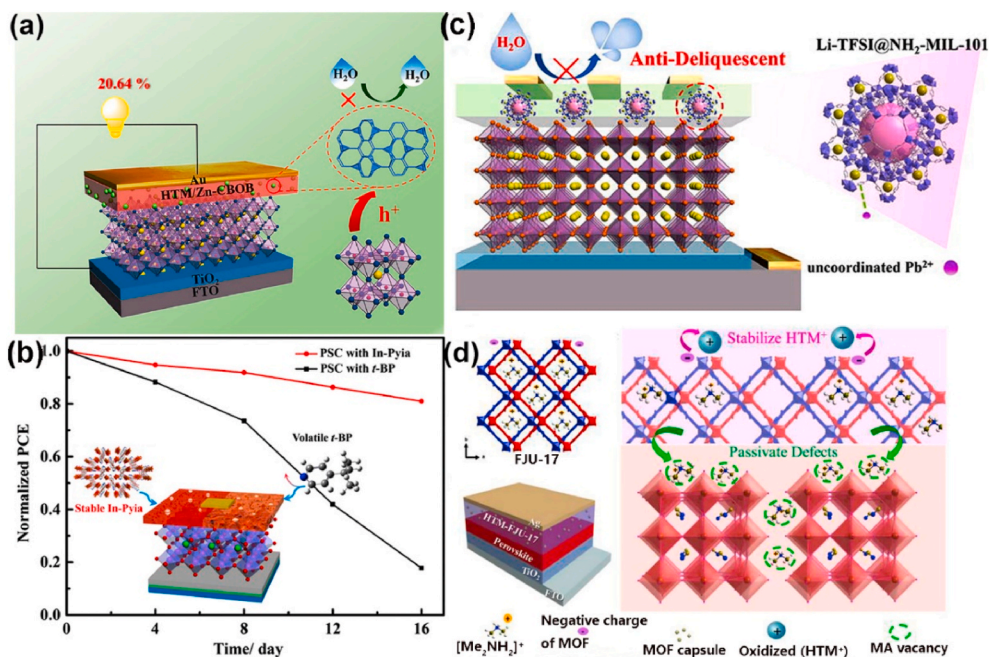


Fig. 5. (a) Schematic diagram and function of Zn-CBOB-doped PSCs [48]. (b) The time-depended PCE decay curves of the devices and molecular structures of H₂Pyia and t-BP [49]. (c) Schematic illustration of the Li-TFSI@NH₂-MIL-101 and function as HTL [77]. (d) FJU-17, schematic diagram of PSCs, and image of defect passivation and hole mobility enhancement induced by the HTM-FJU-17 [50].

Table 3

Summary of the photovoltaic performance of MOFs-modified HTL of PSCs.

MOF	Device structure	Jsc (mA/cm ²)	Voc (V)	FF (%)	PCE (%)	Ref.
[In ₂ (phen) ₃ Cl ₆] · CH ₃ CN·2H ₂ O (In2)	FTO/bl-TiO ₂ /meso-TiO ₂ /Perovskite/Spiro-OMeTAD-In2/Au	21.03	1.01	74	15.8	[46]
[In _{0.5} K(3-q)Cl _{1.5} (H ₂ O) _{0.5}] ₂ n (In10)	FTO/TiO ₂ /Perovskite/Spiro-OMeTAD-In10/Au	24.3	1.0	70	17.0	[71]
[Cu ₂ (BTC) ₄ /3(H ₂ O) ₂] ₆ [H ₃ PMo ₁₂ O ₄₀] ₂ (POM@Cu-BTC)	FTO/TiO ₂ /PCBM/Perovskite/Spiro-OMeTAD-POM@Cu-BTC/Au	23.9	1.11	80	21.44	[47]
Zn-CBOB	FTO/PEDOT: PSS/perovskite/HTM/Zn-CBOB/Au	23.17	1.135	78.4	20.64	[48]
Pb-MOF	FTO/TiO ₂ /Perovskite/Spiro-OMeTAD-Pb-MOF/Au	19.57	1.0	67.3	13.17	[73]
[In(HPyia)Cl ₂] · CH ₃ CN (In-Pyia)	FTO/TiO ₂ /Perovskite/Spiro-OMeTAD-In-Pyia/Au	23.53	1.09	79	20.26	[49]
NH ₂ -MIL-101	FTO/TiO ₂ /PC ₆₁ BM/perovskite/Spiro-OMeTAD-Li-TFSI@NH ₂ -MIL-101/Au	23.41	1.073	75.7	19.01	[77]
FJU-17	FTO/TiO ₂ /perovskite/FJU-17/Ag	25.09	1.05	77	20.34	[50]
Cu-Ni-BTC	FTO/compact layer/mesoporous layer/perovskite/NiO@CuO/Au	21.8	0.91	51	10.11	[78]

framework-8 (ZIF-8) as the interlayer between the compact TiO₂ and perovskite layers (Fig. 6 (a)). Enhanced perovskite grain crystallinity, larger grains, and considerably improved photovoltaic performance (PCE of 16.8%) [81]. Bioki et al. introduced incorporating a thin film of HKUST-1 MOF as an interfacial layer on ETL (mp-TiO₂) of a PSC. The mp-TiO₂ layer has excellent stability and chemical compatibility. Its surface-rich hydroxyl group can connect the precursors of MOFs, providing an excellent heterogeneous nucleation site for HKUST-1 grains. The device shows maximum efficiency of 14.64%, and 65% of its initial efficiency retains after 600 h [82]. Ji and co-workers introduced a polyethyleneimine ethoxylated (PEIE) composite film and tellurophene-based 2D MOF at the ETL and perovskite layer interface to realize the nondestructive passivation of TiO₂. Schematic diagram of the structures of PSCs with and without the PEIE-2D MOF modified layer as shown in Fig. 5 (b). This interfacial layer can recognize the effective passivation of TiO₂ and further improve the morphology of the perovskite film. The device finally achieves highly efficient and stable PSCs with a maximum efficiency of 22.22%, and the modified PSCs retained 83% of their initial efficiency after 84 h [83].

Secondly, MOFs were introduced between the perovskite and HTL layers, which may effectively passivate perovskite surface defects. Nguyen and co-workers synthesized MOF-derived NiO@C nanoparticles and subsequently used them as adequate interference layers between the

perovskite and Spiro-OMeTAD layers in planar n-i-p PSCs. The number of defects at the perovskite surface was reduced, and charge transfer was more efficient, leading to the improved power conversion efficiency of the PSCs. The maximum PCE of PSC was 15.78% [51]. Li and co-workers introduced multifunctional capsules containing ZIF-8 encapsulation agent and ammonium iodide salts as interlayers between the perovskite and HTL. Fig. 6 (c) shows that in the capsule interlayer, ammonium iodide salts in ZIF-8 pores are released to the perovskite layer, compensating for the vacancies. ZIF-8 also prevents the evaporation of the organic component in perovskite and isolates perovskite from moisture. Consequently, the ZIF-8@FAI shows the highest efficiency of 19.13% [84]. Li et al. synthesized a MOF ([{(Me₂NH₂)₃(SO₄)₂][Zn₂(ox)₃]_n, ZnL) and incorporated it into PSCs as an interlayer between the perovskite and HTL for enhancing photovoltaic performance and stability of PSCs devices. As shown in Fig. 6 (d), extensive theoretical calculations and experimental studies confirm the passivation ability of ZnL that amine-containing cations could effectively passivate negatively charged defects, and the anionic framework with dense oxygen sites forms strong interaction with anchoring the atoms of perovskite. As a result, the PSC device shows improved efficiency from 19.75% to 21.15%, and the operational stability of ZnL-based PSCs is significantly improved by 93%, retaining their original PCE after 3000 h of storage [52].

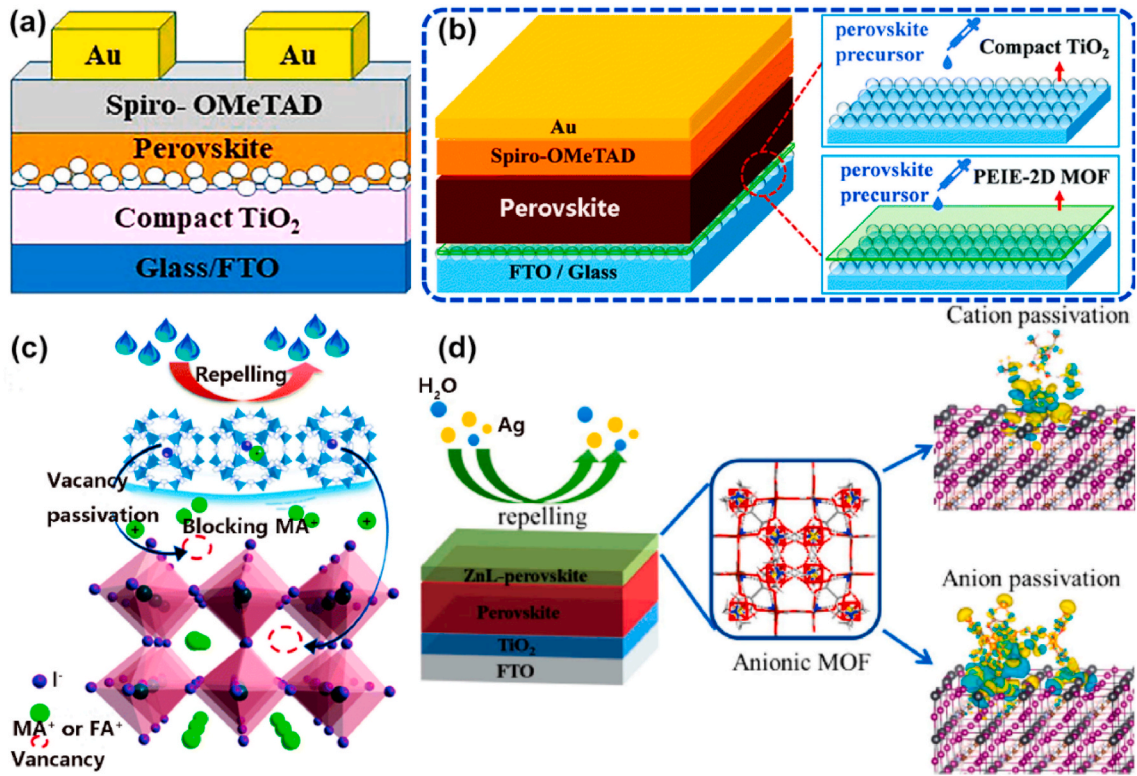


Fig. 6. (a) Schematic illustration of the solar cell device, while ZIF-8 is applied at the c-TiO₂ and perovskite layers [81]. (b) Schematic diagram of the structures of PSCs with and without the PEIE-2D MOF modified layer [83]. (c) Schematic illustration of the effect of ZIF-8@ammonium iodide capsule on perovskite [84]. (d) Structure and multifunction of ZnL-MOF [52].

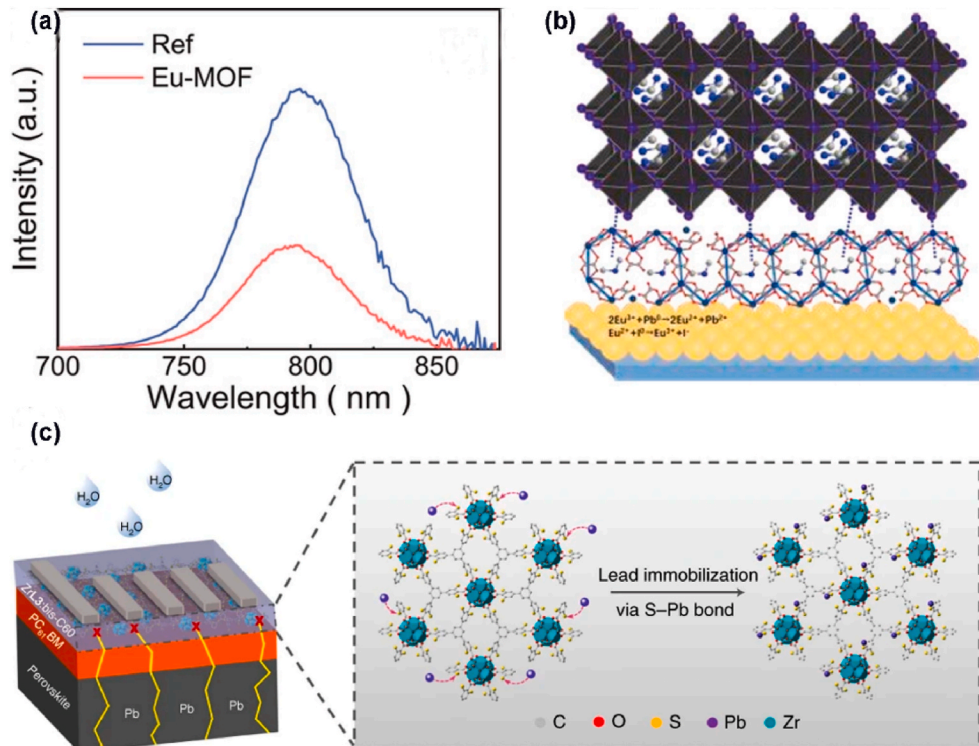


Fig. 7. (a,b) The steady-state PL spectroscopy and schematic illustration of the Eu-MOF effect on perovskite film [53]. (c) Schematic of the degradation process of PVCs and the immobilization effect of ZrL3 on leaked Pb²⁺ ions [29].

At present, the relationship between MOFs modification and residual stress distribution of perovskite films lacks system research. Dou and co-workers introduced an ultrathin Eu-MOF layer at the interface between the perovskite layer to improve the device stability. They analyzed the steady-state PL spectroscopy of FTO/SnO₂/perovskite films (Fig. 7(a)), the PL intensity with Eu-MOF treatment was much lower than the reference one. Fig. 7 (b) exhibited the schematic illustration of the Eu-MOF effect on perovskite film. The Eu-MOF could reduce the defects, improve carrier transport and light utilization, and prevent the decomposition of perovskite under ultraviolet light. Meanwhile, the treatment of Eu-MOF also turned the tensile strain into compressive strain in the perovskite films. Taking the above-mentioned merits of Eu-MOF, the final device exhibits a champion PCE of 22.16%. Moreover, the devices retain 96% of their initial PCE after 2000 h storage with a relative humidity of 30% and 91% of their initial PCE after 1200 h with continuous thermal annealing at 85 °C in the N₂ atmosphere [53].

Moreover, we all know that perovskite materials are straightforward to degrade, resulting in water-dissolved heavy metal lead ions (Pb²⁺) leakage from the degraded perovskite absorbers. MOF is regarded as a promising material for removing metal ions/harmful biological species [85]. Wu and co-workers introduced a thiol-functionalized 2D conjugated MOF as an electron-extraction layer (EEL) at the perovskite/cathode interface. The 2D conjugated MOF used Zr (IV) ions to engage selectively. The complex carboxyl groups allow dense free-standing thiol arrays to be built around the Zr (IV)-oxo cluster to capture most of the Pb²⁺ leaked from the degraded PSCs by forming water-insoluble solids. Unlike the physical encapsulation approaches to reduce the lead leakage, this in-situ chemical adsorption of Pb²⁺ by ZrL₃: bis-C₆₀ EEL in the device is a much more effective and sustainable process for long-term practical applications (Fig. 7 (c)). The resultant devices exhibit high PCEs (22.02%) along with a substantially improved long-term operational stability (over 90% of its initial efficiency for 1000 h at 85 °C.) [29]. This report provides general research ideas for applying functionalized MOF in PSCs. The photovoltaic parameters of the MOFs-modified interface engineering of PSCs are shown in Table 4. At this stage, MOFs as a stable buffer layer in PSCs have obtained promising results due to increased crystallinity of perovskite material or enhanced the charge collection efficiency at the device interface. In addition, the specifically designed MOF molecule can strongly interact with Pb ions, significantly suppressing Pb leakage in the device.

5. MOFs/perovskite heterojunction of PSCs

The perovskite/MOF heterojunction applications have also made significant progress in recent years. Interestingly, the articles reported indicate that using MOFs in the perovskite could enhance the charge-extraction efficiency, inhibit the charge recombination, improve the film quality, and enhance the resulting device stability. Catch up with this emerging material; we will introduce more details of the recent representative progress in the following sections. Chang and co-workers synthesized Zr-based porphyrin metal-organic framework (MOF-525) nanocrystals (a crystal size of about 140 nm) and incorporated them into

PSCs (Fig. 8 (a)). The small MOF-525 nanocrystals incorporated near the bottom of the MOF/perovskite composite thin film act as a regular scaffold to allow perovskite crystallization inside; the standard scaffold provides an ordered order arrangement of perovskite crystallites during the initial stage of crystallization. The morphology and crystallinity of the obtained perovskite thin film can be significantly enhanced. Besides, due to the insulated nature of used MOFs, they believe that the perovskite thin films remain direct bandgap property after adding nanocrystals of MOFs as an additive. The optimal device shows a PCE of 12%. This is the first MOF/perovskite heterojunction report in PSCs [28].

In addition, the MOF material has a conjugated framework, which could filter ultraviolet light. Lee and co-workers introduced two Zr-based MOFs (UiO-66 and MOF-808) into the perovskite absorbing layer and successfully prepared MOFs-modified perovskite heterojunction. Intense absorption in the UV region could filter the UV radiation, which has been cited as harmful for perovskite materials. The hybrid MOFs were found to passivate the grain boundaries of perovskite possibly. Meanwhile, their 3D porous architecture could accommodate small perovskite nanocrystals and provide decent charge-transporting pathways through the MOF scaffolds. The J-V curve and structure of the device as shown in Fig. 8 (b). The PCEs of the UiO-66/MOF-808-hybrid PSCs are further enhanced to 18.01% 17.81%, respectively. Besides, over 70% of the initial PCE is retained after being stored in air (25 °C and relative humidity of 60 ± 5%) for over two weeks [30]. They demonstrated that the perovskite/MOF heterojunctions have tremendous potential for fabricating efficient and stable PSCs.

Mahsa and co-workers introduced three metal-organic compounds of Zr (IV), In (III), and Zn (II) into the perovskite layer to control the crystallization and film formation. The hydroxyl and carboxyl groups in pyda and pydcH₂ ligands interact with ions to influence perovskite films' growth mechanism and quality. Therefore, the PCE of PSCs achieved more than 90% improvement after adding two wt% of zinc MOF as an additive in HTM-free conditions [86]. Then, they used iron terephthalate MOF (MOF-235) to prepare and modify the perovskite layer by the one-step solution method. The device shows a PCE of 9.56% [87]. Very recently, Zhou and co-workers incorporated perovskite with microporous indium-based MOF [In₁₂O(OH)₁₆(H₂O)₅(btc)₆]_n(In-BTC) nanocrystals and formed a heterojunction light-harvesting layer (Fig. 9 (a)). The interconnected micropores and terminal oxygen sites of In-BTC allow the preferential crystallization of perovskite inside the regular cavities, endowing the derived films with improved morphology/crystallinity and reduced grain boundaries/defects. Consequently, the In-BTC-modified PSCs show a PCE of 20.87%. Over 80% of the original PCE is retained after 12 days of exposure to the ambient environment (25 °C and relative humidity of ~65%) without encapsulation [88].

Recent studies have demonstrated that A-site cations with π -conjugated aromatic tails enable tuning the perovskite frontier orbital, reconfiguring the band edge states, and thereby adjusting the electronic-dimensional configuration [89–91]. MOFs with π -conjugated organic groups and an ultra-stable structure can tackle instability issues (moisture and thermal) [92]. Lee and co-workers incorporated a π -conjugated aromatic structure-based MOF (terpyridyl chromium (Cr-MOF)) as

Table 4
Summary of the photovoltaic performance of MOFs-involved interface engineering of PSCs.

MOF	Device structure	Jsc (mA/cm ²)	Voc (V)	FF (%)	PCE (%)	Ref.
ZIF-8	FTO/c-TiO ₂ /m-TiO ₂ /ZIF-8/perovskite/Spiro-OMeTAD/Au	22.82	1.02	73	16.99	[79]
ZIF-8	FTO/c-TiO ₂ /m-TiO ₂ /ZIF-8/perovskite/Spiro-OMeTAD/Ag	19.8	0.972	62	12.0	[80]
ZIF-8	FTO/c-TiO ₂ /ZIF-8/perovskite/Spiro-OMeTAD/Au	21.8	1.23	59	16.8	[81]
HKUST-1	FTO/c-TiO ₂ /mp-TiO ₂ /HKUST-1/perovskite/CuPc/Au	22.75	0.99	65	14.64	[82]
PEIE-2D MOF	FTO/c-TiO ₂ /PEIE-2D MOF/perovskite/Spiro-OMeTAD/Ag	25.36	1.11	79	22.22	[83]
Ni-BTC	FTO/c-TiO ₂ /mp-TiO ₂ /perovskite/NiO@C/Spiro-OMeTAD/Au	22.39	1.02	69.24	15.78	[51]
{[(Me ₂ NH ₂) ₃ (SO ₄) ₂][Zn ₂ (ox) ₃]} _n , ZnL	FTO/TiO ₂ /perovskite/ZnL/HTM/Ag	23.86	1.12	79.3	21.15	[52]
ZIF-8@FAI	FTO/TiO ₂ /perovskite/ZIF-8@FAI/HTM/Ag	23.93	1.06	75.6	19.13	[84]
Eu-MOF	ITO/SnO ₂ /Eu-MOF/perovskite/Spiro-OMeTAD/Au	23.71	1.14	82	22.16	[53]
2D MOF ZrL ₃	ITO/PTAA/perovskite/PC ₆₁ BM/ZrL ₃ : bis-C ₆₀ /Ag	22.58	1.20	81.28	22.02	[29]

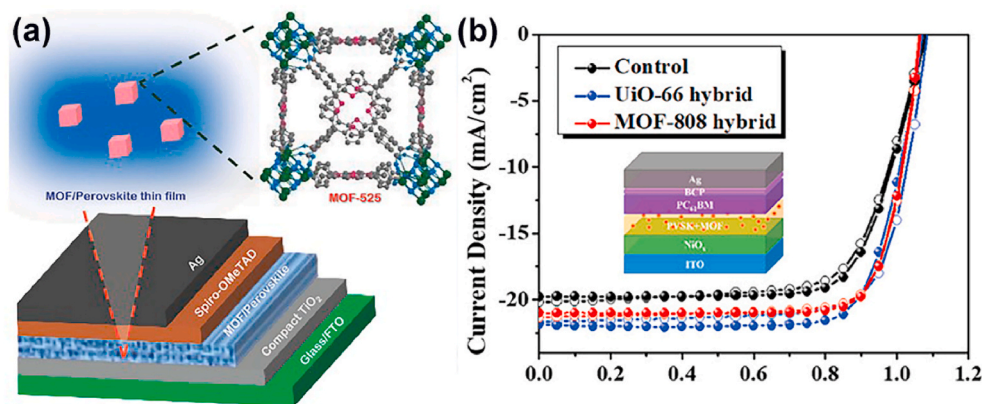


Fig. 8. (a) MOF-525 nanocrystals with a crystal size of about 140 nm are synthesized and incorporated into perovskite solar cells [28]. (b) J–V curves of PSCs with the perovskite/MOF heterojunction and device structure diagram [30].

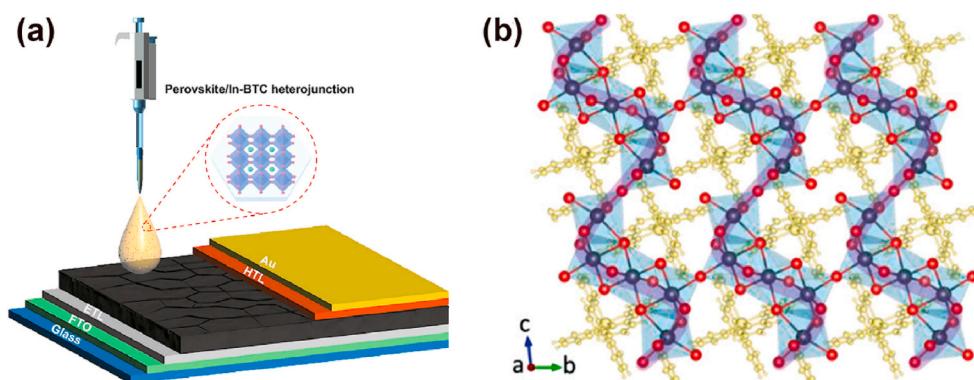


Fig. 9. (a) The schematic diagram for fabricating n-i-p PSCs with the perovskite/In-BTC heterojunction as a light-harvesting layer [88]. (b) Crystal structure of the Cr-MOF perovskite along the (100) lattice plane [90].

A-site cation within the Pb–I framework and successfully constructed a new 2D perovskite crystal structure. Crystal structure of the Cr-MOF perovskite along the (100) lattice plane as shown in Fig. 9 (b). The Cr-MOF perovskite was demonstrated to enhance the device's stability against heat and moisture effectively. Besides, the A-site Cr-MOF group with a π -conjugated structure was proved to habilitate multiple channels for charge-carrier transport between organic conjugated groups and inorganic $[\text{PbI}_6]^{4-}$ octahedra, which significantly improved the perovskite charge transport properties. As a result, the optimized all-inorganic PSCs yield a PCE as high as 17.02%. Remarkably, the stabilized device retains 80% of its PCE after 1000 h in the ambient atmosphere [90]. The photovoltaic parameters of the MOFs-modified perovskite heterojunction of PSCs are shown in Table 5. In summary, the perovskite/MOFs heterojunction has improved ambient stability of PSCs. Meanwhile most of the MOFs can absorb UV-light due to the wider bandgap, which provides valuable research ideas of filtering the UV-light for perovskite photo-active layer for future development.

6. Challenges and prospective

PSCs have outstanding photoelectric characteristics with the PCE on par with single-crystal silicon solar cells. However, the PSCs suffer from the long-term operation-condition instability issue since they are susceptible to moisture, temperature, oxygen, chemicals, and UV illumination. Moreover, perovskite materials undergo large-scale ion migration under external light illumination or electric fields resulting in various vacancies and defects in the perovskite film, consequently reducing the film's photoelectric properties and stability. The application of MOFs in the PSCs can significantly suppress the ion migration, reduce the defect concentration, improve charge-carrier transport and promote charge transfer, resulting in enhanced long-term stability and improved photovoltaic performance. Although noticeable progress has been made in MOFs-assisted perovskite photovoltaics, there are still several challenges in this new type of optoelectronic device, (1) MOFs with a three-dimensional rigid framework are still complicated to realize long-range charge transport. Thus, it is challenging to utilize MOFs as

Table 5
Summary of the photovoltaic performance of MOFs-modified perovskite heterojunction of PSCs.

Structure	Device structure	Jsc (mA/cm ²)	Voc (V)	FF (%)	PCE (%)	Ref.
MOF-525	FTO/c-TiO ₂ /MOF-525/perovskite/Spiro-OMeTAD/Ag	23.04	0.93	60	12.0	[28]
UiO-66	ITO)/NiOx/UiO-66- perovskite/PC ₆₁ BM/BCP/Ag	21.85	1.07	76.9	17.81	[30]
MOF-808	ITO)/NiOx/MOF-808- perovskite/PC ₆₁ BM/BCP/Ag	21.01	1.06	79.8	18.01	[30]
[pyda.H] [Zn(pydc) ₂]. H ₂ O/CH ₃ OH	ITO/TiO ₂ /perovskite-Zn-MOF/Au	9.36	0.96	62	5.64	[86]
MOF-235	ITO/TiO ₂ /perovskite- MOF-235/Spiro-OMeTAD/Au	14.09	1.03	65	9.56	[87]
[In ₁₂ O(OH) ₁₆ (H ₂ O) ₅ (btc) ₆] _n	FTO/c-TiO ₂ /PC ₆₁ BM/perovskite/In-BTC/Spiro-OMeTAD/Au.	23.55	1.12	79	20.87	[88]
Cr-MOF	FTO/NiOx/Cr-MOF-CsPbI ₂ Br/ZnO@C ₆₀ /Ag	16.51	1.30	79	17.02	[90]

photoactive materials in PSCs directly. (2) The application of diverse functional MOFs in PSCs is still less with poor investigation. (3) The influence mechanism of MOFs with different pore diameters on perovskite film formation is still unclear. Moreover, (4) how the MOFs can stabilize perovskites in an ambient environment warrants further investigation from both a kinetic and thermodynamic point of view. Although there are many challenges in the combined use of MOF and PSCs, it does not affect the rapid development of this emerging field.

Through the above-mentioned existing challenges, we propose that the future development trend should focus on the following points:

- (1) MOFs can introduce different functional groups with rich functions due to their porous nanostructure. Each component of PSC can use the unique characteristics of this structure for innovative research, which will be an exciting attempt.
- (2) MOFs' bandgap and semiconducting properties can be adjusted by selecting electron-rich metal nodes/organic molecules based on conjugates, functionalizing organic linkers with electron-donating groups, and increasing the conjugation of organic linkers. The optimal energy level MOF is selected and applied to the device to prepare complete MOF-based PSCs.
- (3) MOFs' porous nature and versatility have good potential for lead leakage sequestration in perovskite film, restricting the release of heavy metal ions to external environments.
- (4) According to previous reports, the proper pore size is critical in PSCs. However, to the best of our knowledge, there is no article yet to explore the application of MOF with different sizes of pores in PSCs and explain the growth mechanism of perovskite in MOF micropores. Solving these problems has important guiding significance for developing MOF/perovskite heterojunction.
- (5) In addition, we believe that the particle size of the MOFs has an equally significant impact on the perovskite. Large particle size MOFs may cause low-quality perovskite film formation. It is also of great significance to explore the application of different particle sizes of MOF in perovskite materials.
- (6) Most of the reported MOFs applied in PSCs are based on classic structures which have been widely reported. Motivated by stronger interaction with Pb ions, better charge carrier transport, more suitable energy bandgap, facile synthesis process with low-cost, designing MOFs materials with novel structures in PSCs will be another future development trend.

Although the MOF/perovskite composites are still in their infancy, they have become prominent in scientific research and device engineering. We believe that the application of MOF-based materials in PSCs will receive more attention and achievements, significantly accelerating the development of this intersecting field.

Declaration of competing interest

The authors declare that they have no known competing financial interests or personal relationships that could have appeared to influence the work reported in this paper.

Acknowledgment

The financial support from the National Natural Science Foundation of China (51472189; 62004129; 22005202) is gratefully acknowledged, and Shenzhen Polytechnic also supported this work.

References

- [1] M. Kim, J. Jeong, H. Lu, T.K. Lee, F.T. Eickemeyer, Y. Liu, I.W. Choi, S.J. Choi, Y. Jo, H.-B. Kim, S.-I. Mo, Y.-K. Kim, H. Lee, N.G. An, S. Cho, W.R. Tress, S. M. Zakeeruddin, A. Hagfeldt, J.Y. Kim, M. Grätzel, D.S. Kim, Conformal quantum dot-SnO₂ layers as electron transporters for efficient perovskite solar cells, *Science* 80 (2022) 302–306, <https://doi.org/10.1126/science.abh1885>, 375.
- [2] Z. Dai, S.K. Yadavalli, M. Chen, A. Abbaspourtamijani, Y. Qi, N.P. Padture, Interfacial toughening with self-assembled monolayers enhances perovskite solar cell reliability, *Science* 80 (2021) 618–622, <https://doi.org/10.1126/science.abf5602>, 372.
- [3] Z. Yao, Z. Xu, W. Zhao, J. Zhang, H. Bian, Y. Fang, Y. Yang, S. (Frank) Liu, Enhanced efficiency of inorganic CsPbI_{3-x}Br_x perovskite solar cell via self-regulation of antisite defects, *Adv. Energy Mater.* 11 (2021), 2100403, <https://doi.org/10.1002/aenm.202100403>.
- [4] J. Zhu, S. Park, O.Y. Gong, C. Sohn, Z. Li, Z. Zhang, B. Jo, W. Kim, G.S. Han, D. H. Kim, T.K. Ahn, J. Lee, H.S. Jung, Formamidinium disulfide oxidant as a localised electron scavenger for > 20% perovskite solar cell modules, *Energy Environ. Sci.* 14 (2021) 4903–4914, <https://doi.org/10.1039/D1EE01440D>.
- [5] Q. Zhou, J. Duan, J. Du, Q. Guo, Q. Zhang, X. Yang, Y. Duan, Q. Tang, Tailored lattice “tape” to confine tensile interface for 11.08%-efficiency all-inorganic CsPbBr₃ perovskite solar cell with an ultrahigh voltage of 1.702 V, *Adv. Sci.* 8 (2021), 2101418, <https://doi.org/10.1002/adv.202101418>.
- [6] D. Thakur, S.-E. Chiang, M.-H. Yang, J.-S. Wang, S.H. Chang, Self-stability of un-encapsulated polycrystalline MAPbI₃ solar cells via the formation of chemical bonds between C₆₀ molecules and MA cations, *Sol. Energy Mater. Sol. Cells* 235 (2022), 111454, <https://doi.org/10.1016/j.solmat.2021.111454>.
- [7] D.H. Kim, J.B. Whitaker, Z. Li, M.F.A.M. van Hest, K. Zhu, Outlook and challenges of perovskite solar cells toward terawatt-scale photovoltaic module technology, *Joule* 2 (2018) 1437–1451, <https://doi.org/10.1016/j.joule.2018.05.011>.
- [8] M. Saliba, J.-P. Correa-Baena, M. Grätzel, A. Hagfeldt, A. Abate, Perovskite solar cells: from the atomic level to film quality and device performance, *Angew. Chem. Int. Ed.* 57 (2018) 2554–2569, <https://doi.org/10.1002/anie.201703226>.
- [9] L. Xie, P. Song, L. Shen, J. Lu, K. Liu, K. Lin, W. Feng, C. Tian, Z. Wei, Revealing the compositional effect on the intrinsic long-term stability of perovskite solar cells, *J. Mater. Chem. A* 8 (2020) 7653–7658, <https://doi.org/10.1039/D0TA01668C>.
- [10] C.-Y. Chang, C.-C. Wang, Enhanced stability and performance of air-processed perovskite solar cells via defect passivation with a thiazole-bridged diketopyrrolopyrrole-based π -conjugated polymer, *J. Mater. Chem. A* 8 (2020) 8593–8604, <https://doi.org/10.1039/D0TA00978D>.
- [11] X. Zhang, T. Wu, X. Xu, L. Zhang, J. Tang, X. He, J. Wu, Z. Lan, Ligand-exchange TiO₂ nanocrystals induced formation of high-quality electron transporting layers at low temperature for efficient planar perovskite solar cells, *Sol. Energy Mater. Sol. Cells* 178 (2018) 65–73, <https://doi.org/10.1016/j.solmat.2018.01.021>.
- [12] Y. Hou, J. Yang, Q. Jiang, W. Li, Z. Zhou, X. Li, S. Zhou, Enhancement of photovoltaic performance of perovskite solar cells by modification of the interface between the perovskite and mesoporous TiO₂ film, *Sol. Energy Mater. Sol. Cells* 155 (2016) 101–107, <https://doi.org/10.1016/j.solmat.2016.05.004>.
- [13] H. Wang, S. Li, X. Liu, Z. Shi, X. Fang, J. He, Low-dimensional metal halide perovskite photodetectors, *Adv. Mater.* 33 (2021), 2003309, <https://doi.org/10.1002/adma.202003309>.
- [14] N.K. Tailor, Y. Yukta, R. Ranjan, S. Ranjan, T. Sharma, A. Singh, A. Garg, K.S. Nalwa, R.K. Gupta, S. Satapathi, The effect of dimensionality on the charge carrier mobility of halide perovskites, *J. Mater. Chem. A* 9 (2021) 21551–21575, <https://doi.org/10.1039/D1TA03749H>.
- [15] T. Niu, L. Chao, W. Gao, C. Ran, L. Song, Y. Chen, L. Fu, W. Huang, Ionic liquids-enabled efficient and stable perovskite photovoltaics: progress and challenges, *ACS Energy Lett.* (2021) 1453–1479, <https://doi.org/10.1021/acsenenergylett.0c02696>.
- [16] J. Sun, X. Zhang, X. Ling, Y. Yang, Y. Wang, J. Guo, S. (Frank) Liu, J. Yuan, W. Ma, A penetrated 2D/3D hybrid heterojunction for high-performance perovskite solar cells, *J. Mater. Chem. A* 9 (2021) 23019–23027, <https://doi.org/10.1039/D1TA06514A>.
- [17] M.A. Mahmud, T. Duong, J. Peng, Y. Wu, H. Shen, D. Walter, H.T. Nguyen, N. Mozaffari, G.D. Tabi, K.R. Catchpole, K.J. Weber, T.P. White, Origin of efficiency and stability enhancement in high-performing mixed dimensional 2D-3D perovskite solar cells: a review, *Adv. Funct. Mater.* 32 (2022), 2009164, <https://doi.org/10.1002/adfm.202009164>.
- [18] Y. Cheng, L. Ding, Pushing commercialization of perovskite solar cells by improving their intrinsic stability, *Energy Environ. Sci.* 14 (2021) 3233–3255, <https://doi.org/10.1039/D1EE00493J>.
- [19] G. Tong, D.-Y. Son, L.K. Ono, H.-B. Kang, S. He, L. Qiu, H. Zhang, Y. Liu, J. Hieulle, Y. Qi, Removal of residual compositions by powder engineering for high efficiency formamidinium-based perovskite solar cells with operation lifetime over 2000 h, *Nano Energy* 87 (2021), 106152, <https://doi.org/10.1016/j.nanoen.2021.106152>.
- [20] C. Luo, G. Zheng, F. Gao, X. Wang, Y. Zhao, X. Gao, Q. Zhao, Facet orientation tailoring via 2D-seed-induced growth enables highly efficient and stable perovskite solar cells, *Joule* 6 (2022) 240–257, <https://doi.org/10.1016/j.joule.2021.12.006>.
- [21] M.F. Mohamad Noh, N.A. Arzaee, I.N. Nawas Mumthas, N.A. Mohamed, S.N. F. Mohd Nasir, J. Safaei, A.R. bin, M. Yusoff, M.K. Nazeeruddin, M.A. Mat Teridi, High-humidity processed perovskite solar cells, *J. Mater. Chem. A* 8 (2020) 10481–10518, <https://doi.org/10.1039/D0TA01178A>.
- [22] W. Xiang, S. (Frank) Liu, W. Tress, A review on the stability of inorganic metal halide perovskites: challenges and opportunities for stable solar cells, *Energy Environ. Sci.* 14 (2021) 2090–2113, <https://doi.org/10.1039/D1EE00157D>.
- [23] Y. Zhou, I. Poli, D. Meggiolaro, F. De Angelis, A. Petrozza, Defect activity in metal halide perovskites with wide and narrow bandgap, *Nat. Rev. Mater.* 6 (2021) 986–1002, <https://doi.org/10.1038/s41578-021-00331-x>.
- [24] C. Liu, Y. Yang, K. Rakstys, A. Mahata, M. Franckevicius, E. Mosconi, R. Skackauskaite, B. Ding, K.G. Brooks, O.J. Usiobo, J.-N. Audinot, H. Kanda, S. Driukas, G. Kavaliauskaitė, V. Gulbinas, M. Dessimov, V. Getautis, F. De Angelis, Y. Ding, S. Dai, P.J. Dyson, M.K. Nazeeruddin, Tuning structural isomers of phenylenediammonium to afford efficient and stable perovskite solar cells and

- modules, *Nat. Commun.* 12 (2021) 6394, <https://doi.org/10.1038/s41467-021-26754-2>.
- [25] S. Song, E.Y. Park, B.S. Ma, D.J. Kim, H.H. Park, Y.Y. Kim, S.S. Shin, N.J. Jeon, T. Kim, J. Seo, Selective defect passivation and topographical control of 4-dimethylaminopyridine at grain boundary for efficient and stable planar perovskite solar cells, *Adv. Energy Mater.* 11 (2021), 2003382, <https://doi.org/10.1002/aenm.202003382>.
- [26] A.R. bin Mohd Yusoff, M. Vasilopoulou, D.G. Georgiadou, L.C. Palilis, A. Abate, M. K. Nazeeruddin, Passivation and process engineering approaches of halide perovskite films for high efficiency and stability perovskite solar cells, *Energy Environ. Sci.* 14 (2021) 2906–2953, <https://doi.org/10.1039/D1EE00062D>.
- [27] D.-H. Kang, C. Ma, N.-G. Park, Antiseptic povidone-iodine heals the grain boundary of perovskite solar cells, *ACS Appl. Mater. Interfaces* (2022), <https://doi.org/10.1021/acsami.1c21479> acsami.1c21479.
- [28] T.-H. Chang, C.-W. Kung, H.-W. Chen, T.-Y. Huang, S.-Y. Kao, H.-C. Lu, M.-H. Lee, K.M. Boopathi, C.-W. Chu, K.-C. Ho, Planar heterojunction perovskite solar cells incorporating metal-organic framework nanocrystals, *Adv. Mater.* 27 (2015) 7229–7235, <https://doi.org/10.1002/adma.201502537>.
- [29] S. Wu, Z. Li, M.Q. Li, Y. Diao, F. Lin, T. Liu, J. Zhang, P. Tieu, W. Gao, F. Qi, X. Pan, Z. Xu, Z. Zhu, A.K.Y. Jen, 2D metal-organic framework for stable perovskite solar cells with minimized lead leakage, *Nat. Nanotechnol.* 15 (2020) 934–940, <https://doi.org/10.1038/s41565-020-0765-7>.
- [30] C.-C. Lee, C.-I. Chen, Y.-T. Liao, K.C.-W. Wu, C.-C. Chueh, Enhancing efficiency and stability of photovoltaic cells by using perovskite/Zr-MOF heterojunction including bilayer and hybrid structures, *Adv. Sci.* 6 (2019), 1801715, <https://doi.org/10.1002/adv.201801715>.
- [31] S. Xie, W. Monnens, K. Wan, W. Zhang, W. Guo, M. Xu, I.F.J. Vanketlecom, X. Zhang, J. Fransaer, Cathodic electrodeposition of MOF films using hydrogen peroxide, *Angew. Chem. Int. Ed.* (2021), <https://doi.org/10.1002/anie.202108485>.
- [32] Q. Wang, D. Astruc, State of the art and prospects in metal-organic framework (MOF)-Based and MOF-derived nanocatalysis, *Chem. Rev.* 120 (2020) 1438–1511, <https://doi.org/10.1021/acs.chemrev.9b00223>.
- [33] B. Zhang, Y. Zheng, T. Ma, C. Yang, Y. Peng, Z. Zhou, M. Zhou, S. Li, Y. Wang, C. Cheng, Designing MOF nanoarchitectures for electrochemical water splitting, *Adv. Mater.* 33 (2021), 2006042, <https://doi.org/10.1002/adma.202006042>.
- [34] H. Fan, M. Peng, I. Strauss, A. Mundstock, H. Meng, J. Caro, MOF-in-COF molecular sieving membrane for selective hydrogen separation, *Nat. Commun.* 12 (2021) 38, <https://doi.org/10.1038/s41467-020-20298-7>.
- [35] W. Meng, S. Kondo, T. Ito, K. Komatsu, Y. Pirillo, Y. Hijikata, Y. Ikuhara, T. Aida, H. Sato, An elastic metal-organic crystal with a densely catenated backbone, *Nature* 598 (2021) 298–303, <https://doi.org/10.1038/s41586-021-03880-x>.
- [36] W. Cheng, H. Zhang, D. Luan, X.W. (David) Lou, Exposing unsaturated Cu₁-O₂ sites in nanoscale Cu-MOF for efficient electrocatalytic hydrogen evolution, *Sci. Adv.* 7 (2021), <https://doi.org/10.1126/sciadv.abg2580>.
- [37] H. Wang, H. Zou, Y. Liu, Z. Liu, W. Sun, K.A. Lin, T. Li, S. Luo, Ni₂P nanocrystals embedded Ni-MOF nanosheets supported on nickel foam as bifunctional electrocatalyst for urea electrolysis, *Sci. Rep.* (2021) 1–11, <https://doi.org/10.1038/s41598-021-00776-8>.
- [38] A. Sharma, J. Lim, S. Jeong, S. Won, J. Seong, S. Lee, Y.S. Kim, S. Bin Baek, M. S. Lah, Superprotonic conductivity of MOF-808 achieved by controlling the binding mode of grafted sulfamate, *Angew. Chem. Int. Ed.* 60 (2021) 14334–14338, <https://doi.org/10.1002/anie.202103191>.
- [39] Y. Zou, Y. Huang, D. Si, Q. Yin, Q. Wu, Z. Weng, R. Cao, Porous metal-organic framework liquids for enhanced CO₂ adsorption and catalytic conversion, *Angew. Chem.* 133 (2021) 21083–21088, <https://doi.org/10.1002/ange.202107156>.
- [40] S. Ehrling, E.M. Reynolds, V. Bon, I. Senkovska, T.E. Gorelik, J.D. Evans, M. Rauche, M. Mendt, M.S. Weiss, A. Pöpl, E. Brunner, U. Kaiser, A.L. Goodwin, S. Kaskel, Adaptive response of a metal-organic framework through reversible disorder-disorder transitions, *Nat. Chem.* 13 (2021) 568–574, <https://doi.org/10.1038/s41557-021-00684-4>.
- [41] J. Nicks, K. Sasitharan, R.R.R. Prasad, D.J. Ashworth, J.A. Foster, Metal-organic framework nanosheets: programmable 2D materials for catalysis, sensing, electronics, and separation applications, *Adv. Funct. Mater.* 31 (2021), 2103723, <https://doi.org/10.1002/adfm.202103723>.
- [42] C.-C. Chueh, C.-I. Chen, Y.-A. Su, H. Konnerth, Y.-J. Gu, C.-W. Kung, K.C.-W. Wu, Harnessing MOF materials in photovoltaic devices: recent advances, challenges, and perspectives, *J. Mater. Chem. A* 7 (2019) 17079–17095, <https://doi.org/10.1039/C9TA03595H>.
- [43] A.V. Vinogradov, H. Zaahe-Hertling, E. Hey-Hawkins, A.V. Agafonov, G. A. Seisenbaeva, V.G. Kessler, V.V. Vinogradov, The first depleted heterojunction TiO₂-MOF-based solar cell, *Chem. Commun.* 50 (2014) 10210–10213, <https://doi.org/10.1039/C4CC01978D>.
- [44] X. Hou, L. Pan, S. Huang, O.-Y. Wei, X. Chen, Enhanced efficiency and stability of perovskite solar cells using porous hierarchical TiO₂ nanostructures of scattered distribution as scaffold, *Electrochim. Acta* 236 (2017) 351–358, <https://doi.org/10.1016/j.electacta.2017.03.192>.
- [45] Y.-N. Zhang, B. Li, L. Fu, Q. Li, L.-W. Yin, MOF-derived ZnO as electron transport layer for improving light harvesting and electron extraction efficiency in perovskite solar cells, *Electrochim. Acta* 330 (2020), 135280, <https://doi.org/10.1016/j.electacta.2019.135280>.
- [46] M. Li, D. Xia, Y. Yang, X. Du, G. Dong, A. Jiang, R. Fan, Doping of [In₂(phen)₃Cl₆]·CH₃CN·2H₂O indium-based metal-organic framework into hole transport layer for enhancing perovskite solar cell efficiencies, *Adv. Energy Mater.* 8 (2018), 1702052, <https://doi.org/10.1002/aenm.201702052>.
- [47] Y. Dong, J. Zhang, Y. Yang, L. Qiu, D. Xia, K. Lin, J. Wang, X. Fan, R. Fan, Self-assembly of hybrid oxidant POM@Cu-btc for enhanced efficiency and long-term stability of perovskite solar cells, *Angew. Chem. Int. Ed.* 58 (2019) 17610–17615, <https://doi.org/10.1002/anie.201909291>.
- [48] J. Wang, J. Zhang, Y. Yang, S. Gai, Y. Dong, L. Qiu, D. Xia, X. Fan, W. Wang, B. Hu, W. Cao, R. Fan, New insight into the Lewis basic sites in metal-organic framework-doped hole transport materials for efficient and stable perovskite solar cells, *ACS Appl. Mater. Interfaces* 13 (2021) 5235–5244, <https://doi.org/10.1021/acsami.0c19968>.
- [49] X. Zhou, L. Qiu, R. Fan, H. Ye, C. Tian, S. Hao, Y. Yang, Toward high-efficiency and thermally-stable perovskite solar cells: a novel metal-organic framework with active pyridyl sites replacing 4-tert-butylpyridine, *J. Power Sources* 473 (2020), 228556, <https://doi.org/10.1016/j.jpowsour.2020.228556>.
- [50] J. Zhang, S. Guo, M. Zhu, C. Li, J. Chen, L. Liu, S. Xiang, Z. Zhang, Simultaneous defect passivation and hole mobility enhancement of perovskite solar cells by incorporating anionic metal-organic framework into hole transport materials, *Chem. Eng. J.* 408 (2021), 127328, <https://doi.org/10.1016/j.cej.2020.127328>.
- [51] T.M. Huyen Nguyen, C.W. Bark, Highly porous nanostructured NiO/C as interface-effective layer in planar n-i-p perovskite solar cells, *J. Alloys Compd.* 841 (2020), 155711, <https://doi.org/10.1016/j.jallcom.2020.155711>.
- [52] C. Li, J. Qiu, M. Zhu, Z. Cheng, J. Zhang, S. Xiang, X. Zhang, Z. Zhang, Multifunctional anionic metal-organic frameworks enhancing stability of perovskite solar cells, *Chem. Eng. J.* (2021), 133587, <https://doi.org/10.1016/j.cej.2021.133587>.
- [53] J. Dou, C. Zhu, H. Wang, Y. Han, S. Ma, X. Niu, N. Li, C. Shi, Z. Qiu, H. Zhou, Y. Bai, Q. Chen, Synergistic effects of Eu-MOF on perovskite solar cells with improved stability, *Adv. Mater.* 33 (2021), 2102947, <https://doi.org/10.1002/adma.202102947>.
- [54] H. Lu, W. Tian, B. Gu, Y. Zhu, L. Li, TiO₂ electron transport bilayer for highly efficient planar perovskite solar cell, *Small* 13 (2017), 1701535, <https://doi.org/10.1002/smll.201701535>.
- [55] M.M. Byrnavand, T. Kim, S. Song, G. Kang, S.U. Ryu, T. Park, p-Type CuI islands on TiO₂ electron transport layer for a highly efficient planar-perovskite solar cell with negligible hysteresis, *Adv. Energy Mater.* 8 (2018), 1702235, <https://doi.org/10.1002/aenm.201702235>.
- [56] H. Lu, J. Zhong, C. Ji, J. Zhao, D. Li, R. Zhao, Y. Jiang, S. Fang, T. Liang, H. Li, C. M. Li, Fabricating an optimal rutile TiO₂ electron transport layer by delicately tuning TiCl₄ precursor solution for high performance perovskite solar cells, *Nano Energy* 68 (2020), 104336, <https://doi.org/10.1016/j.nanoen.2019.104336>.
- [57] B. Li, J. Zhao, Q. Lu, S. Zhou, H. Wei, T. Lv, Y. Zhang, J. Zhang, Q. Liu, Carbon-based printable perovskite solar cells with a mesoporous TiO₂ electron transporting layer derived from metal-organic framework NH₂-MIL-125, *Energy Technol.* 9 (2021), 2000957, <https://doi.org/10.1002/ente.202000957>.
- [58] Y.-H. Liao, Y.-H. Chang, T.-H. Lin, S.-H. Chan, K.-M. Lee, K.-H. Hsu, J.-F. Hsu, M.-C. Wu, Boosting the power conversion efficiency of perovskite solar cells based on Sn doped TiO₂ electron extraction layer via modification the TiO₂ phase junction, *Sol. Energy* 205 (2020) 390–398, <https://doi.org/10.1016/j.solener.2020.05.039>.
- [59] T.M.H. Nguyen, C.W. Bark, Synthesis of cobalt-doped TiO₂ based on metal-organic frameworks as an effective electron transport material in perovskite solar cells, *ACS Omega* 5 (2020) 2280–2286, <https://doi.org/10.1021/acsomega.9b03507>.
- [60] U. Ryu, S. Jee, J.-S. Park, I.K. Han, J.H. Lee, M. Park, K.M. Choi, Nanocrystalline titanium metal-organic frameworks for highly efficient and flexible perovskite solar cells, *ACS Nano* 12 (2018) 4968–4975, <https://doi.org/10.1021/acsnano.8b02079>.
- [61] J. Ma, J. Su, Z. Lin, L. Zhou, J. He, J. Zhang, S. Liu, J. Chang, Y. Hao, Improve the oxide/perovskite heterojunction contact for low temperature high efficiency and stable all-inorganic CsPbI₂Br perovskite solar cells, *Nano Energy* 67 (2020), 104241, <https://doi.org/10.1016/j.nanoen.2019.104241>.
- [62] M. Shen, Y. Zhang, H. Xu, H. Ma, MOFs based on the application and challenges of perovskite solar cells, *iScience* 24 (2021) 103069, <https://doi.org/10.1016/j.isci.2021.103069>.
- [63] X. Lian, J. Chen, S. Shan, G. Wu, H. Chen, Polymer modification on the NiO_x hole transport layer boosts open-circuit voltage to 1.19 V for perovskite solar cells, *ACS Appl. Mater. Interfaces* 12 (2020) 46340–46347, <https://doi.org/10.1021/acsami.0c11731>.
- [64] X. Ding, H. Wang, C. Chen, H. Li, Y. Tian, Q. Li, C. Wu, L. Ding, X. Yang, M. Cheng, Passivation functionalized phenothiazine-based hole transport material for highly efficient perovskite solar cell with efficiency exceeding 22%, *Chem. Eng. J.* 410 (2021), 128328, <https://doi.org/10.1016/j.cej.2020.128328>.
- [65] N. Yaghoobi Nia, M. Zendehele, M. Abdi-Jalebi, L.A. Castriotta, F.U. Kosasih, E. Lamanna, M.M. Abolhasani, Z. Zheng, Z. Andaji-Garmaroudi, K. Asadi, G. Divitini, C. Ducati, R.H. Friend, A. Di Carlo, Beyond 17% stable perovskite solar module via polaron arrangement of tuned polymeric hole transport layer, *Nano Energy* 82 (2021), 105685, <https://doi.org/10.1016/j.nanoen.2020.105685>.
- [66] G.M. Arumugam, S.K. Karunakaran, C. Liu, C. Zhang, F. Guo, S. Wu, Y. Mai, Inorganic hole transport layers in inverted perovskite solar cells: a review, *Nano Sel.* 2 (2021) 1081–1116, <https://doi.org/10.1002/nano.202000200>.
- [67] G. Kim, H. Choi, M. Kim, J. Lee, S.Y. Son, T. Park, Hole transport materials in conventional structural (n-i-p) perovskite solar cells: from past to the future, *Adv. Energy Mater.* 10 (2020), 1903403, <https://doi.org/10.1002/aenm.201903403>.
- [68] Y. Liu, Y. Hu, X. Zhang, P. Zeng, F. Li, B. Wang, Q. Yang, M. Liu, Inhibited aggregation of lithium salt in Spiro-OMeTAD toward highly efficient perovskite solar cells, *Nano Energy* 70 (2020), 104483, <https://doi.org/10.1016/j.nanoen.2020.104483>.
- [69] A. Barranco, M.C. Lopez-Santos, J. Idigoras, F.J. Aparicio, J. Obrero-Perez, V. Lopez-Flores, L. Contreras-Bernal, V. Rico, J. Ferrer, J.P. Espinos, A. Borrás, J.

- A. Anta, J.R. Sanchez-Valencia, Enhanced stability of perovskite solar cells incorporating dopant-free crystalline spiro-OMeTAD layers by vacuum sublimation, *Adv. Energy Mater.* 10 (2020), 1901524, <https://doi.org/10.1002/aenm.201901524>.
- [70] J.-Y. Seo, H.-S. Kim, S. Akin, M. Stojanovic, E. Simon, M. Fleischer, A. Hagfeldt, S. M. Zakeeruddin, M. Grätzel, Novel p-dopant toward highly efficient and stable perovskite solar cells, *Energy Environ. Sci.* 11 (2018) 2985–2992, <https://doi.org/10.1039/C8EE01500G>.
- [71] M. Li, J. Wang, A. Jiang, D. Xia, X. Du, Y. Dong, P. Wang, R. Fan, Y. Yang, Metal organic framework doped Spiro-OMeTAD with increased conductivity for improving perovskite solar cell performance, *Sol. Energy* 188 (2019) 380–385, <https://doi.org/10.1016/j.solener.2019.05.078>.
- [72] Y. Dong, J. Zhang, Y. Yang, J. Wang, B. Hu, W. Wang, W. Cao, S. Gai, D. Xia, K. Lin, R. Fan, Multifunctional nanostructured host-guest POM@MOF with lead sequestration capability induced stable and efficient perovskite solar cells, *Nano Energy* 97 (2022), 107184, <https://doi.org/10.1016/j.nanoen.2022.107184>.
- [73] L. Huang, X. Zhou, R. Wu, C. Shi, R. Xue, J. Zou, C. Xu, J. Zhao, W. Zeng, Oriented haloing metal-organic framework providing high efficiency and high moisture-resistance for perovskite solar cells, *J. Power Sources* 433 (2019), 226699, <https://doi.org/10.1016/j.jpowsour.2019.226699>.
- [74] Y. Hua, B. Xu, P. Liu, H. Chen, H. Tian, M. Cheng, L. Kloo, L. Sun, High conductivity Ag-based metal organic complexes as dopant-free hole-transport materials for perovskite solar cells with high fill factors, *Chem. Sci.* 7 (2016) 2633–2638, <https://doi.org/10.1039/C5SC03569D>.
- [75] J. Xia, R. Zhang, J. Luo, H. Yang, H. Shu, H.A. Malik, Z. Wan, Y. Shi, K. Han, R. Wang, X. Yao, C. Jia, Dipole evoked hole-transporting material p-doping by utilizing organic salt for perovskite solar cells, *Nano Energy* 85 (2021), 106018, <https://doi.org/10.1016/j.nanoen.2021.106018>.
- [76] T. Wu, R. Zhuang, R. Zhao, R. Zhao, L. Zhu, G. Liu, R. Wang, K. Zhao, Y. Hua, Understanding the effects of fluorine substitution in lithium salt on photovoltaic properties and stability of perovskite solar cells, *ACS Energy Lett.* 6 (2021) 2218–2228, <https://doi.org/10.1021/acsenenergylett.1c00685>.
- [77] J. Wang, J. Zhang, Y. Yang, Y. Dong, W. Wang, B. Hu, J. Li, W. Cao, K. Lin, D. Xia, R. Fan, Li-TFSI endohedral Metal-Organic frameworks in stable perovskite solar cells for Anti-Deliquescent and restricting ion migration, *Chem. Eng. J.* 429 (2022), 132481, <https://doi.org/10.1016/j.cej.2021.132481>.
- [78] F. Hazeghi, S. Mozaffari, S.M.B. Ghorashi, Metal organic framework-derived core-shell CuO@NiO nanospheres as hole transport material in perovskite solar cell, *J. Solid State Electrochem.* 24 (2020) 1427–1438, <https://doi.org/10.1007/s10008-020-04643-w>.
- [79] D. Shen, A. Pang, Y. Li, J. Dou, M. Wei, Metal-organic frameworks at interfaces of hybrid perovskite solar cells for enhanced photovoltaic properties, *Chem. Commun.* 54 (2018) 1253–1256, <https://doi.org/10.1039/C7CC09452C>.
- [80] H. Chung, C. Lin, S. Prabu, H. Wang, Perovskite solar cells using TiO₂ layers coated with metal-organic framework material ZIF-8, *J. Chin. Chem. Soc.* 65 (2018) 1476–1481, <https://doi.org/10.1002/jccs.201800173>.
- [81] M.-R. Ahmadian-Yazdi, N. Gholampour, M. Eslamian, Interface engineering by employing zeolitic imidazolate framework-8 (ZIF-8) as the only scaffold in the architecture of perovskite solar cells, *ACS Appl. Energy Mater.* 3 (2020) 3134–3143, <https://doi.org/10.1021/acsaem.9b02115>.
- [82] H. Amrollahi Bioki, A. Moshaii, M. Borhani Zarandi, Performance improvement of ambient-condition fabricated perovskite solar cells using an interfacial HKUST-1 MOF on electron transfer layer, *Surface. Interfac.* 27 (2021), 101579, <https://doi.org/10.1016/j.surf.2021.101579>.
- [83] J. Ji, B. Liu, H. Huang, X. Wang, L. Yan, S. Qu, X. Liu, H. Jiang, M. Duan, Y. Li, M. Li, Nondestructive passivation of the TiO₂ electron transport layer in perovskite solar cells by the PEIE-2D MOF interfacial modified layer, *J. Mater. Chem. C* 9 (2021) 7057–7064, <https://doi.org/10.1039/D1TC00036E>.
- [84] C. Li, S. Guo, J. Chen, Z. Cheng, M. Zhu, J. Zhang, S. Xiang, Z. Zhang, Mitigation of vacancy with ammonium salt-trapped ZIF-8 capsules for stable perovskite solar cells through simultaneous compensation and loss inhibition, *Nanoscale Adv.* 3 (2021) 3554–3562, <https://doi.org/10.1039/D1NA00173F>.
- [85] P. Sharma, V.K. Shahi, Assembly of MIL-101(Cr)-sulphonated poly(ether sulfone) membrane matrix for selective electrodialytic separation of Pb²⁺ from mono-/bi-valent ions, *Chem. Eng. J.* 382 (2020), 122688, <https://doi.org/10.1016/j.cej.2019.122688>.
- [86] M. Seifpanah Sowmehsaraee, M. Ranjbar, M. Abedi, S.A. Mozaffari, Fabrication of lead iodide perovskite solar cells by incorporating zirconium, indium and zinc metal-organic frameworks, *Sol. Energy* 214 (2021) 138–148, <https://doi.org/10.1016/j.solener.2020.12.001>.
- [87] M.S. Sowmehsaraee, M. Abedi, M. Ranjbar, Incorporating MOF-235 in lead iodide perovskite solar cell and investigating its efficiency and stability, *J. Mater. Sci. Mater. Electron.* 32 (2021) 15143–15150, <https://doi.org/10.1007/s10854-021-06064-5>.
- [88] X. Zhou, L. Qiu, R. Fan, J. Zhang, S. Hao, Y. Yang, Heterojunction incorporating perovskite and microporous metal-organic framework nanocrystals for efficient and stable solar cells, *Nano-Micro Lett.* 12 (2020) 80, <https://doi.org/10.1007/s40820-020-00417-1>.
- [89] J. Xue, R. Wang, X. Chen, C. Yao, X. Jin, K.-L. Wang, W. Huang, T. Huang, Y. Zhao, Y. Zhai, D. Meng, S. Tan, R. Liu, Z.-K. Wang, C. Zhu, K. Zhu, M.C. Beard, Y. Yan, Y. Yang, Reconfiguring the band-edge states of photovoltaic perovskites by conjugated organic cations, *Science* 80 (2021) 636–640, <https://doi.org/10.1126/science.abd4860>, 371.
- [90] S. Yuan, Y. Xian, Y. Long, A. Cabot, W. Li, J. Fan, Chromium-based metal-organic framework as A-site cation in CsPbI₂Br perovskite solar cells, *Adv. Funct. Mater.* (2021), 2106233, <https://doi.org/10.1002/adfm.202106233>.
- [91] Y. Gao, Z. Wei, P. Yoo, E. Shi, M. Zeller, C. Zhu, P. Liao, L. Dou, Highly stable lead-free perovskite field-effect transistors incorporating linear π -conjugated organic ligands, *J. Am. Chem. Soc.* 141 (2019) 15577–15585, <https://doi.org/10.1021/jacs.9b06276>.
- [92] Z. Jin, J. Yan, X. Huang, W. Xu, S. Yang, D. Zhu, J. Wang, Solution-processed transparent coordination polymer electrode for photovoltaic solar cells, *Nano Energy* 40 (2017) 376–381, <https://doi.org/10.1016/j.nanoen.2017.08.028>.